


RESEARCH

Open Access



Evaluation of pathological response to neoadjuvant chemotherapy in locally advanced cervical cancer

Li-Jun Wei^{1,2†}, Jia Fu^{1,2†}, Hai-Xia Yang^{1,3†}, Xia Yang^{1,2}, Hao-Yu Liang^{1,2}, Rong-Zhen Luo^{1,2*} and Li-Li Liu^{1,2*} 

Abstract

Neoadjuvant chemotherapy (NACT) is a viable therapeutic option for women diagnosed locally advanced cervical cancer (LACC). However, the factors influencing pathological response are still controversial. We collected pair specimens of 185 LACC patients before and after receiving NACT and conducted histological evaluation. 8 fresh tissues pre-treatment were selected from the entire cohort to conducted immune gene expression profiling. A novel pathological grading system was established by comprehensively assessing the percentages of viable tumor, inflammatory stroma, fibrotic stroma, and necrosis in the tumor bed. Then, 185 patients were categorized into either the good pathological response (GPR) group or the poor pathological response (PPR) group post-NACT, with 134 patients (72.4%, 134/185) achieving GPR. Increasing tumor-infiltrating lymphocytes (TILs) and tumor-infiltrating lymphocytes volume (TILV) pre-treatment were correlated with GPR, with TILV emerging as an independent predictive factor for GPR. Additionally, CIBERSORT analysis revealed noteworthy differences in the expression of immune makers between cPR and non-cPR group. Furthermore, a significantly heightened density of CD8+T cells and a reduced density of FOXP3+T cells were observed in GPR than PPR. Importantly, patients exhibiting GPR or inflammatory type demonstrated improved overall survival and disease-free survival. Notably, stromal type was an independent prognostic factor in multivariate analysis. Our study indicates the elevated TILV in pre-treatment specimens may predict a favorable response to NACT, while identifying stromal type in post-treatment specimens as an independent prognostic factor. Moreover, we proposed this pathological grading system in NACT patients, which may offer a more comprehensive understanding of treatment response and prognosis.

Keywords Neoadjuvant chemotherapy, Pathological response, Stromal type, Locally advanced cervical cancer, Prognosis

[†]Li-Jun Wei, Jia Fu and Hai-Xia Yang contributed equally to this work.

*Correspondence:
Rong-Zhen Luo
luorzh@sysucc.org.cn
Li-Li Liu
liulil@sysucc.org.cn

¹State Key Laboratory of Oncology in South China, Collaborative Innovation Center for Cancer Medicine, Sun Yat-sen University Cancer Center, Guangzhou 510060, China

²Department of Pathology, Sun Yat-sen University Cancer Center, 651# Dong Feng Road East, Guangzhou 510060, Guangdong, China

³Department of Pathology, The Second Affiliated Hospital of Shenzhen University, Shenzhen 518101, China



© The Author(s) 2024. **Open Access** This article is licensed under a Creative Commons Attribution 4.0 International License, which permits use, sharing, adaptation, distribution and reproduction in any medium or format, as long as you give appropriate credit to the original author(s) and the source, provide a link to the Creative Commons licence, and indicate if changes were made. The images or other third party material in this article are included in the article's Creative Commons licence, unless indicated otherwise in a credit line to the material. If material is not included in the article's Creative Commons licence and your intended use is not permitted by statutory regulation or exceeds the permitted use, you will need to obtain permission directly from the copyright holder. To view a copy of this licence, visit <http://creativecommons.org/licenses/by/4.0/>. The Creative Commons Public Domain Dedication waiver (<http://creativecommons.org/publicdomain/zero/1.0/>) applies to the data made available in this article, unless otherwise stated in a credit line to the data.

Introduction

Cervical cancer is the second most prevalent contributor to both cancer incidence and mortality for women in developing countries [1]. Concurrent chemoradiotherapy (CCRT) is recommended as the treatment for Locally advanced cervical cancer (LACC) [2, 3]. Nevertheless, constraints exist in utilizing CCRT for LACC treatment [4]. Certain studies have reported the utilization of hysterectomy following neoadjuvant chemotherapy (NACT) for LACC, which may reduce tumor sizes, decrease the probability of tumor metastasis and recurrence, rectify pelvic anatomy distortion, ultimately facilitating the enhanced delivery of subsequent therapies [5]. Studies indicate a favorable correlation between superior clinical and pathologic responses to NACT and improved survival rates among LACC patients [6, 7]. Conversely, stable disease post-NACT has also been identified as a harbinger of poor prognosis [8]. Despite NACT being employed globally, consensus guidelines for the optimal patient selection remain elusive.

Previous studies highlight the impact of immune cells in the tumor microenvironment on the efficacy of anti-cancer therapies [9, 10]. Elevated pre-treatment densities of tumor infiltrating lymphocytes (TILs) correlate positively with complete pathological response (cPR) rates [11]. D'Alessandris et al. observed a significant correlation between the percentage of TILs and PD-L1 expression on pathological response to NACT, indicating the robust immunogenic potential of cervical cancer [10]. Existing studies predominantly focused on TILs percentage, but do not take into account the stroma, which may not fully reflect tumor immunity. We found that tumor infiltrating lymphocytes volume (TILV) has demonstrated superior predictive value for cPR and overall survival in triple-negative invasive breast cancer [12]. TILV was calculated by using the formula $TILV = \text{stroma in tumor (\%)} \times \text{stromal TILs (\%)}$, which considered both the percentage of TILs and tumor stroma. However, the predictive and prognostic significance of TILV in cervical cancer remains unexplored.

The histopathologic evaluation of surgical specimens represents an ideal for assessing NACT effectiveness. Although the histopathologic assessment of NACT response is established for various solid tumors (e.g., breast, esophagus and ovarian) [13–15], no universally accepted system exists for cervical cancer. Several studies have quantified residual tumors and chemotherapy-induced regressive changes in other tumors, correlating these with patient outcomes [16, 17]. In cervical cancer, previous studies have proposed some pathological response grading method and morphological changes after neoadjuvant therapy [18, 19]. However, they have not been associated with prognosis, and none have achieved widespread adoption in routine clinical practice

due to differing criterion. This study aimed to establish a simple, prognostically significant, and reproducible grading system of evaluating LACC patients' responses to NACT, based on the examination of resection specimens, and can be incorporated into routine histopathology reporting.

Materials and methods

Patients and samples

The studied cohort were retrospectively retrieved from the pathologic files of Sun Yat-sen University Cancer Center (SYSUCC) between August 1, 2007 and January 31, 2019. Inclusion criteria are as follows: (1) diagnosis of LACC (2018 FIGO stage IB3, IIA2-IVA) from biopsy, including squamous cell carcinomas, adenocarcinomas, adenosquamous carcinoma and neuroendocrine small cell carcinomas. (2) received 1–3 cycles of NACT or neoadjuvant chemotherapy combined with immunotherapy (NACIT). (3) underwent a radical hysterectomy after 3–4 weeks of NACT. Low-grade or high-grade squamous intraepithelial lesion, adenocarcinoma in situ, mesenchymal tumors and germ cell tumors were excluded. Pelvic computed tomography (CT) was performed before NACT and 7–10 days after the last chemotherapeutic course, and the response evaluation criteria in solid tumors (RECIST, v1.1) were applied to score the chemotherapeutic response [20]. Stable disease (SD) refers to <30% decrease or >20% increase in the longest diameter; partial response (PR) refers to >30% decrease in the longest diameter; complete response (CR) refers to tumor complete resolution. Pair specimens of 185 LACC patients before and after receiving NACT were collected, while 7 pair samples before and after receiving NACIT. Both biopsy and resection specimens are available for review on hematoxylin-eosin (H&E) slides. The schematic overview of the study design was shown in Fig. 1A.

Pathological response evaluation

Pathological response after NACT were evaluated on H&E-stained slides of resection specimens by two experienced pathologists. As shown in Fig. 1B, tumor beds refer to the area where the original tumor was believed to be located before treatment, consists of viable tumor, necrosis, stroma including inflammation and fibrosis, and the total of 4 components is 100% [16]. The percentage of every component was made in 5% or 10% increments as continuous variables, unless the amount less than 10%. In this case, an estimate of single-digit percentages should be recorded. Every slide that tumor bed can be recognized was reviewed, as well as each proportion of 4 components was given and then average was taken respectively. As proposed in previous studies [21], pathological responses were classified into 4 categories according to the proportion of residual viable tumor: complete

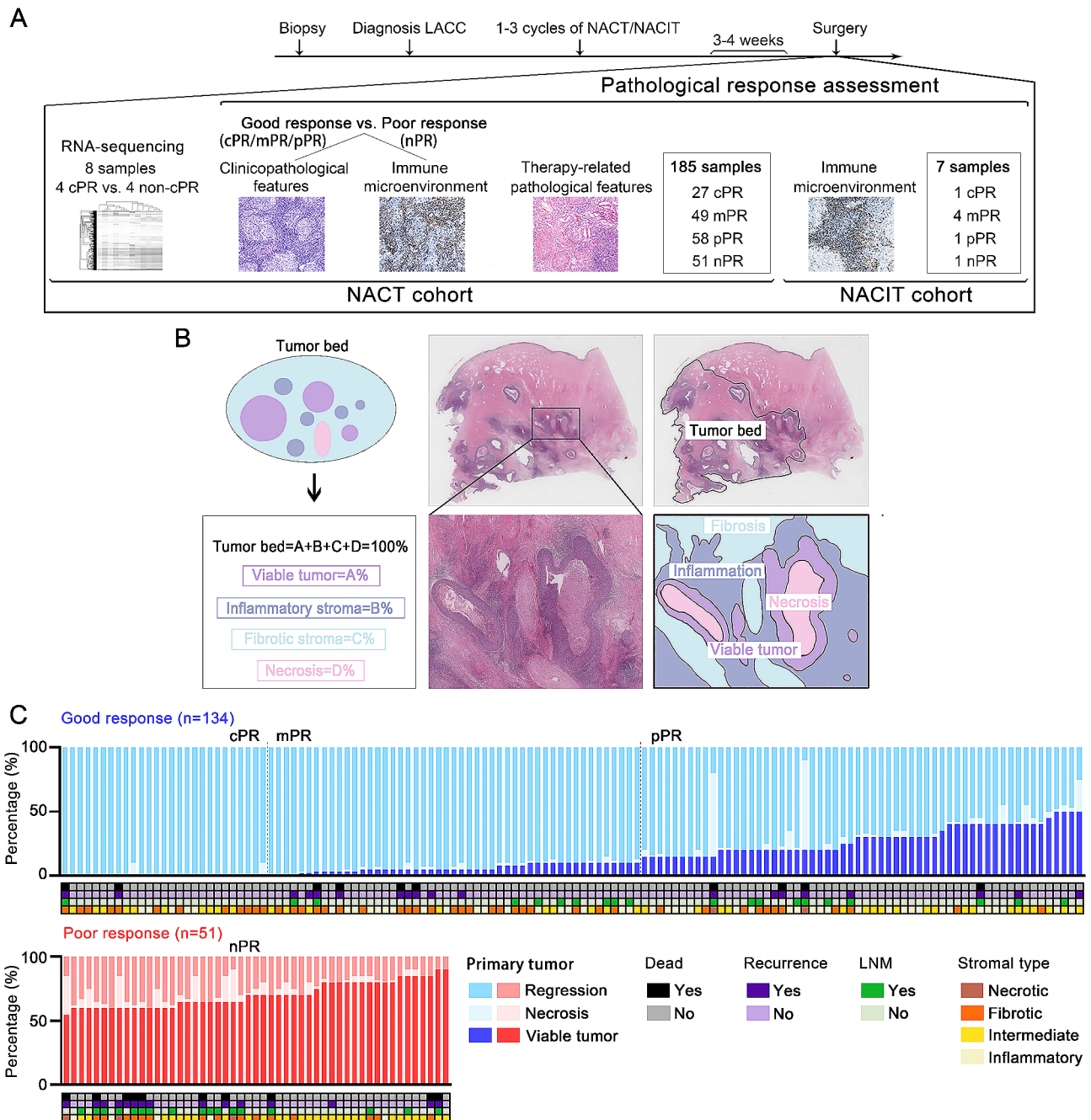


Fig. 1 (A) Schematic overview of the study design. (B) Histological components of tumor bed. (C) Evaluation of viable tumor, regression and necrosis in primary tumor and clinicopathological features in 185 LACC patients. NACT, neoadjuvant chemotherapy; NACIT, neoadjuvant chemotherapy combined with immunotherapy; cPR, complete pathological response; mPR, major pathological response; pPR, partial pathological response; nPR, no pathological response; LNM, Lymph node metastatic

pathological response (cPR) was defined as the absence of viable tumor; major pathological response (mPR) refers to viable tumor >0 but ≤10%; partial pathological response (pPR) refers to viable tumor >10% but ≤50%; no pathological response (nPR) refers to viable tumor >50%. Patients who obtained cPR, mPR and pPR were considered as achieving good pathological response. Patients who were considered as nPR were classified into poor

response group. Then, as shown in Supplementary Figure S2A, we classified the tumor stromal type into 4 categories based on the proportion of 3 components excluding residual viable tumor: inflammatory type, the proportion of inflammatory stroma exceeded that of both fibrotic stroma and necrosis by 10%; fibrotic type, the proportion of fibrotic stroma exceeded that of both inflammatory stroma and necrosis by 10%; necrotic

type, the proportion of necrosis exceeded that of both inflammatory and fibrotic stroma by 10%; intermediate type, the proportion of 3 components differed from each other $\leq 10\%$. The evaluation of TILs and TILV referred to previous guidelines [12, 22].

Differentially expressed genes (DEG) and immune infiltration identification by bioinformatic tools

We selected 8 fresh biopsy tissues pre-treatment (4 cases from cPR group and 4 cases from non-cPR group) from the NACT cohort to conduct RNA sequencing. The RNA sequencing was performed with the help of Beijing Genomics institution. To better identify the DEG and plot them, mRNA levels were normalized as $\log_2(x+1)$. The DEG between indicated different groups were analyzed by the helpful R package *edgeR* (lumina [23]; cluster profiler [24]) to generate a heat map. To note, the cut off for filtering for DEG was fold change > 1 and $p < 0.05$. The differentially expressed genes (DEGs) in the indicated group underwent gene ontology (GO) enrichment analysis using the R package (*cluster profiler*). A level of False Discovery Rates (FDR) < 0.05 was applied to determine statistical significance. Furthermore, to determine the immune cell proportions in tumor tissue samples within the indicated section, we employed the CIBERSORT algorithm [25].

Immunohistochemistry (IHC) staining

Formalin-fixed, paraffin-embedded tumor sections were stained with IHC. Following deparaffinization with xylene and ethanol, each slide was treated with 3% hydrogen peroxide in methanol. The slides were blocked overnight with avidin-biotin at 4 °C, followed by incubation with antibodies against CD8 (ZSGB, ZA-0508), CD4 (ZSGB, ZA-0519), FOXP3 (Abcam, ab20034), PD-L1 (Dako 22C3), and ki-67 (ZSGB, ZA-0502). After washing the slides three times with PBS, biotinylated goat anti-mouse antibodies were incubated, followed by the staining of 3,3'-diaminobenzidine tetrahydro-chloride (DAB) and the counterstaining of Mayer's hematoxylin. Two experienced pathologists observed and evaluated the staining under a microscope. Three high power fields in the peritumor stroma were randomly selected to count the density of CD8+, CD4+ and FOXP3+T cells. PD-L1 expression was assessed using three scoring systems, including combined positive score (CPS), tumor proportion score (TPS) and immune cell proportion score (IPS), according to the PD-L1 measurement criteria [26]. CPS $\geq 1\%$, TPS $\geq 1\%$ and ICS $\geq 1\%$ were considered PD-L1 positive.

Statistical analysis

SPSS 26.0 was used to perform statistical analyses (SPSS, Chicago, IL, USA). Clinicopathological and immune

parameters were divided into high and low groups using the maximum (sensitivity+specificity) point of the Receiver Operating Characteristic (ROC) curve for the prediction of pathological response. Difference of clinicopathological characteristics and PD-L1 expression between groups were determined by Fisher's exact test or Chi-square test. Pathological response and radiological response were correlated using Spearman's test. Kruskal-Wallis test was used to analyze the difference of CD8+, CD4+ and FOXP3+T cells density level between groups. Univariate and multivariate logistic regression analyses were used to analyze clinicopathological features for pathological response. The survival analysis was performed by Kaplan-Meier analysis and compared by log-rank test. The prognostic correlations were analyzed with univariate and multivariate Cox regression analyses. $P < 0.05$ was assumed statistically significant.

Results

Pathological response to NACT

Clinicopathological characteristics and pathological response assessment of the NACT cohort were shown in Fig. 1C. Among the 185 total patients with LACC receiving NACT, spanning ages 19 to 67, 134 patients (72.4%, 134/185) achieved good pathological response, including 27 cPR (14.6%, 27/185), 49 mPR (26.5%, 49/185) and pPR (31.4%, 27/185). Conversely, 51 patients (31.4%, 51/185) exhibited poor pathological response. The representative CT images and H&E staining micrographs illustrating pathological response (cPR, mPR, pPR, nPR) in patients before and after NACT were displayed in Fig. 2A. The accompanying pie chart in Fig. 2B delineates the components of various pathological and radiological response in the NACT cohort. The radiographic objective response rate (CR plus PR) stood at 90.8% (168/185) post-NACT. Furthermore, statistical analysis unveiled a significant correlation between pathological and radiological reductions ($R = 0.355$, $p < 0.001$) (Fig. 2B). Among the 27 patients with cPR, 22.2% (6/27) demonstrated CR, while 77.8% (21/27) exhibited PR. These findings underscore the inadequacy of CT scans for accurately evaluating treatment effectiveness in LACC, emphasizing the imperative need to identify biomarkers capable of predicting the efficacy of NACT.

High TILs and TILV significantly associated with good pathological response

Next, we analyzed the relationship between clinicopathological characteristics and pathological response (Table 1 and Supplementary Table 1). The investigation revealed a significant correlation between pathological response and several key factors, including lymph node metastatic ($p = 0.005$), vascular invasion ($p = 0.017$), TILs ($p = 0.043$) and TILV ($p = 0.025$) (Table 1). However, there were no

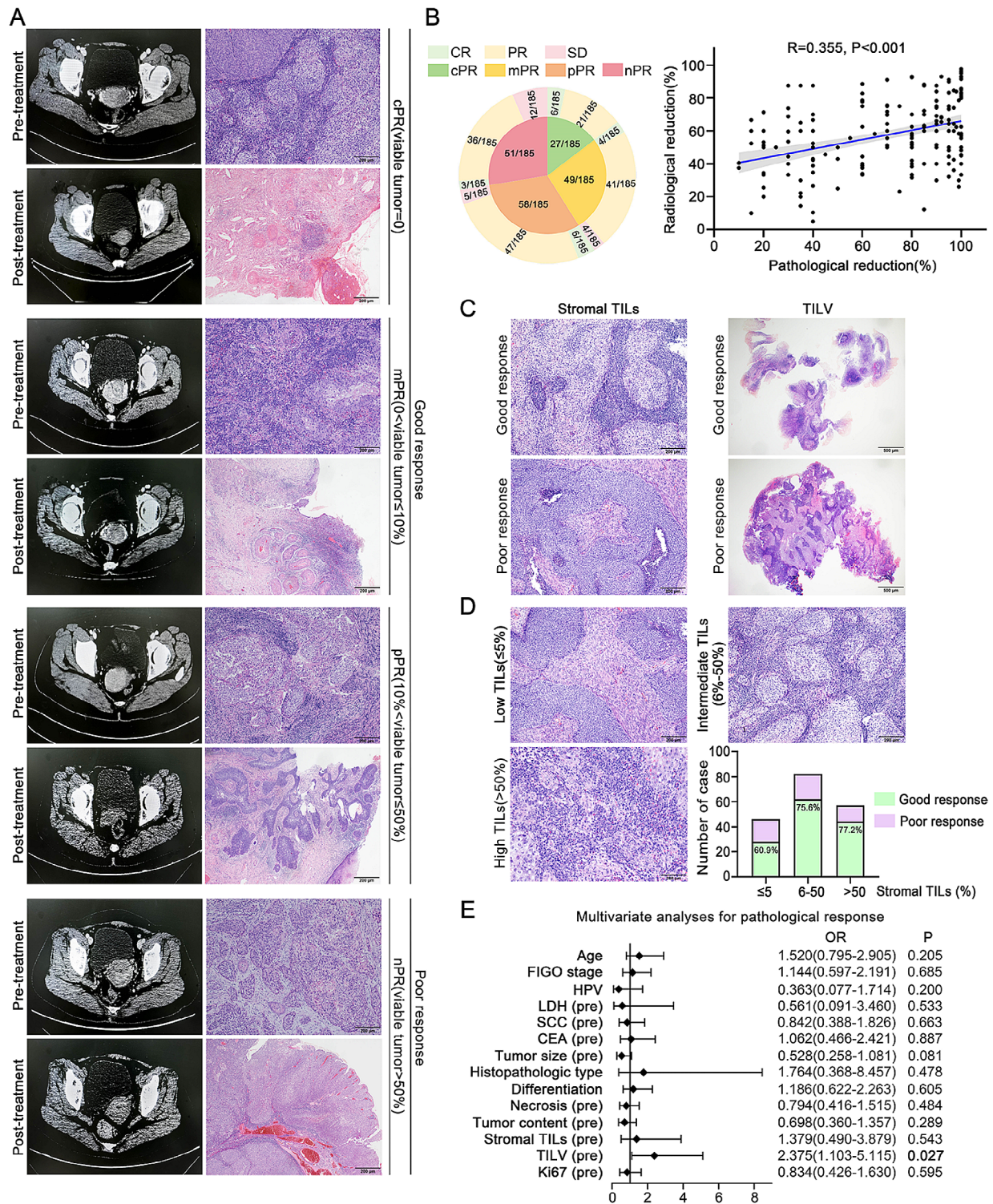


Fig. 2 (A) Representative images of radiological and pathological response pre-treatment and post-treatment. (B) Fractions of patients with their pathological and radiological response in NACT cohort and the correlation analysis between pathological reduction and radiological reduction. (C) Representative images of TILs and TILV, which were associated with pathological response post-treatment. TILV (tumor-infiltrating lymphocytes volume) = stroma proportion (%) × stromal TILs proportion (%) (upper panels: stroma = 30%, stromal TILs = 80%, TILV = 2400; lower panels: stroma = 50%, stromal TILs = 5%, TILV = 250). (D) Representative images and fractions of various grades of stromal TILs, and the correlation with pathological response. (E) Multivariate analyses of clinicopathological features for pathological response are shown in forest map. LACC, locally advanced cervical cancer; cPR, complete pathological response; Proportion of residual tumor; mPR, major pathological response; pPR, partial pathological response; nPR, no pathological response; CR, complete response; PR, partial response; SD, stable disease; TILs, tumor-infiltrating lymphocytes

Table 1 Clinicopathological characteristics of the NACT cohort.

Variables	Total (N, %)	Good response (cPR/mPR/pPR) (N, %)	Poor response (nPR) (N, %)	P
All cases	185	134(72.4)	51(27.6)	
Age (years)				0.898
Median (range)	49.0(19.0–67.0)	49.0(19.0–66.0)	48.0(29.0–67.0)	
FIGO Stage				0.684
IB3	79(42.7)	56(41.8)	23(45.1)	
IIA2-IVA	106(57.3)	78(58.2)	28(54.9)	
Chemotherapy regimen				0.054
Paclitaxel + Cisplatin	87(47.0)	64(47.8)	23(45.1)	
Docetaxel + Cisplatin	70(37.8)	55(41.0)	15(29.4)	
Paclitaxel + Carboplatin	16(8.6)	10(7.5)	6(11.8)	
Others	12(6.5)	5(3.7)	7(13.7)	
Chemotherapy cycles				0.457
1–2	108(58.4)	76(56.7)	32(62.7)	
3	77(41.6)	58(43.3)	19(37.3)	
Adjuvant treatment				0.180
Yes	159(85.9)	118(88.1)	41(80.4)	
No	26(14.1)	16(11.9)	10(19.6)	
Radiological response				0.001
CR	19(10.3)	16(11.9)	3(5.9)	
PR	149(80.5)	112(83.6)	37(72.5)	
SD	17(9.2)	6(4.5)	11(21.6)	
HPV status				0.416
Positive	94(50.8)	66(49.3)	28(54.9)	
Negative	15(8.1)	13(9.7)	2(3.9)	
NA	76(41.1)	55(41.0)	21(41.2)	
Tumor size (pre)(cm)				0.078
>5.9	45(24.3)	28(20.9)	17(33.3)	
≤5.9	140(75.7)	106(79.1)	34(66.7)	
Histologic type				0.473
SCCA	174(94.1)	125(93.3)	49(96.1)	
AC + ASC + NEC	11(5.9)	9(6.7)	2(3.9)	
Differentiation				0.605
Well + Moderate	85(45.9)	60(44.8)	25(49.0)	
Poor	100(54.1)	74(55.2)	26(51.0)	
Parametrium invasion				0.245
Yes	9(4.9)	5(3.7)	4(7.8)	
No	176(95.1)	129(96.3)	47(92.2)	
Lymph node metastatic				0.005
Yes	37(20.0)	20(14.9)	17(33.3)	
No	148(80.0)	114(85.1)	34(66.7)	
Vascular invasion				0.017
Yes	37(20.0)	21(15.7)	16(31.4)	
No	148(80.0)	113(84.3)	35(68.6)	
Nerve bundle invasion				0.103
Yes	10(5.4)	5(3.7)	5(9.8)	
No	175(94.6)	129(96.3)	46(90.2)	
LDH (pre)(u/L)				0.617
>250.0	5(2.7)	3(2.2)	2(3.9)	
≤250.0	180(97.3)	131(97.8)	49(96.1)	
SCC (pre)(ng/ml)				0.662
>1.5	141(76.2)	101(75.4)	40(78.4)	
≤1.5	44(23.8)	33(24.6)	11(21.6)	

Table 1 (continued)

Variables	Total (N, %)	Good response (cPR/mPR/pPR) (N, %)	Poor response (nPR) (N, %)	P
CEA (pre)(ng/ml)				0.946
>5.0	37(20.0)	27(20.1)	10(19.6)	
≤5.0	124(67.0)	89(66.4)	35(68.6)	
NA	24(13.0)	18(13.4)	6(11.8)	
Necrosis (pre)				0.483
Yes	83(44.9)	58(43.3)	25(49.0)	
No	102(55.1)	76(56.7)	26(51.0)	
Tumor content (pre) (%)				0.288
>85	65(35.1)	44(32.8)	21(41.2)	
≤85	120(64.9)	90(67.2)	30(58.8)	
Stromal TILs (pre) (%)				0.043
>5	139(75.1)	106(79.1)	33(64.7)	
≤5	46(24.9)	28(20.9)	18(35.3)	
TILV (pre)				0.025
>75	150(81.1)	114(85.1)	36(70.6)	
≤75	35(18.9)	20(14.9)	15(29.4)	
Ki-67(pre) (%)				0.595
>25	114(61.6)	81(60.4)	33(64.7)	
≤25	71(38.4)	53(39.6)	18(35.3)	

NACT, neoadjuvant chemotherapy; cPR, complete pathological response; mPR, major pathological response; pPR, partial pathological response; nPR, no pathological response; FIGO, International Federation of Gynecology and Obstetrics; HPV, human papilloma virus; NA, not available; LDH, lactate dehydrogenase; SCC, squamous cell carcinoma antigen; CEA, carcinoembryonic antigen; SCCA, squamous cell carcinoma; AC, adenocarcinoma; ASC, adenosquamous carcinoma; NEC, neuroendocrine carcinoma; TILs, tumor-infiltrating lymphocytes; TILV, tumor-infiltrating lymphocytes volume, TILV=stroma proportion (%) × stromal TILs proportion (%). Pre, pre-treatment; Post, post-treatment

statistical connections between pathological response and the remaining clinicopathological parameters, including HPV status and histologic type. Figure 2C illustrated LACC patients who exhibited good pathological response demonstrated a higher prevalence of elevated stromal TILs and TILV. In addition, we observed that a noteworthy 77.2% of patients with high grade of stromal TILs (>50%) achieved good pathological response, surpassing those with low (≤5%) or intermediate (6–50%) grades of stromal TILs (Fig. 2D). Furthermore, upon multivariate analysis, high TILV emerged as an independent predictor for good pathological response (OR=2.375, 95%CI=1.103–5.115, $p=0.027$) in LACC patients (Supplementary Tables 2 and Fig. 2E).

Active tumor immune microenvironment significantly correlated with good pathological response

To compare the tumor immune microenvironment (TIME) characteristics between pathological response of cPR and non-cPR patients, we initially examined immune genes expression in fresh tissues obtained from 4 cases each of cPR and non-cPR. Analysis using CIBERSORT and Kyoto Encyclopedia of Genes and Genomes (KEGG) clustering indicated predominant activation of the human T-cell pathway in the cPR group compared to the non-cPR group (Supplementary Figure S1A-B). Besides, the cPR group exhibited associations with some immune

pathways, including positive regulation of T cell proliferation and mature B cell differentiation (Supplementary Figure S1C). Subsequent analysis focused on the expression of chemokines, chemokine receptors and immune cells in cPR and non-cPR LACC (Fig. 3A-B). According to the correlation analyses among variable immune cells, higher expression of CD8+T cells correlated with lower expression of neutrophils (Fig. 3C). Additionally, the cPR group displayed a higher proportion of CD8+T cells ($p=0.057$), plasma cells ($p=0.029$), and a lower proportion of neutrophils ($p=0.027$) compared to the non-cPR group (Fig. 3D).

Building upon RNA sequencing analyses above, we assessed the density of CD4, CD8, Foxp3 and PD-L1-positive TILs in tumoral stromal tissues from 185 biopsy specimens. As shown in Fig. 3E, the CD8, CD4 and FOXP3 IHC staining results in the same 4 pairs of cases were consistent with the RNA sequencing data. Representative IHC staining images in good response group and poor response group were depicted in Fig. 3F. LACC cases exhibiting good pathological response demonstrated a heightened tendency density of CD8+T cells ($p=0.015$) and a reduced density of FOXP3+T cells ($p=0.036$). In addition, an elevated CD4+/CD8+T cells ratio ($p=0.010$) and an increased CD8+/FOXP3+T cells ratio ($p<0.0001$) was also observed in good response group. No significant differences were observed in

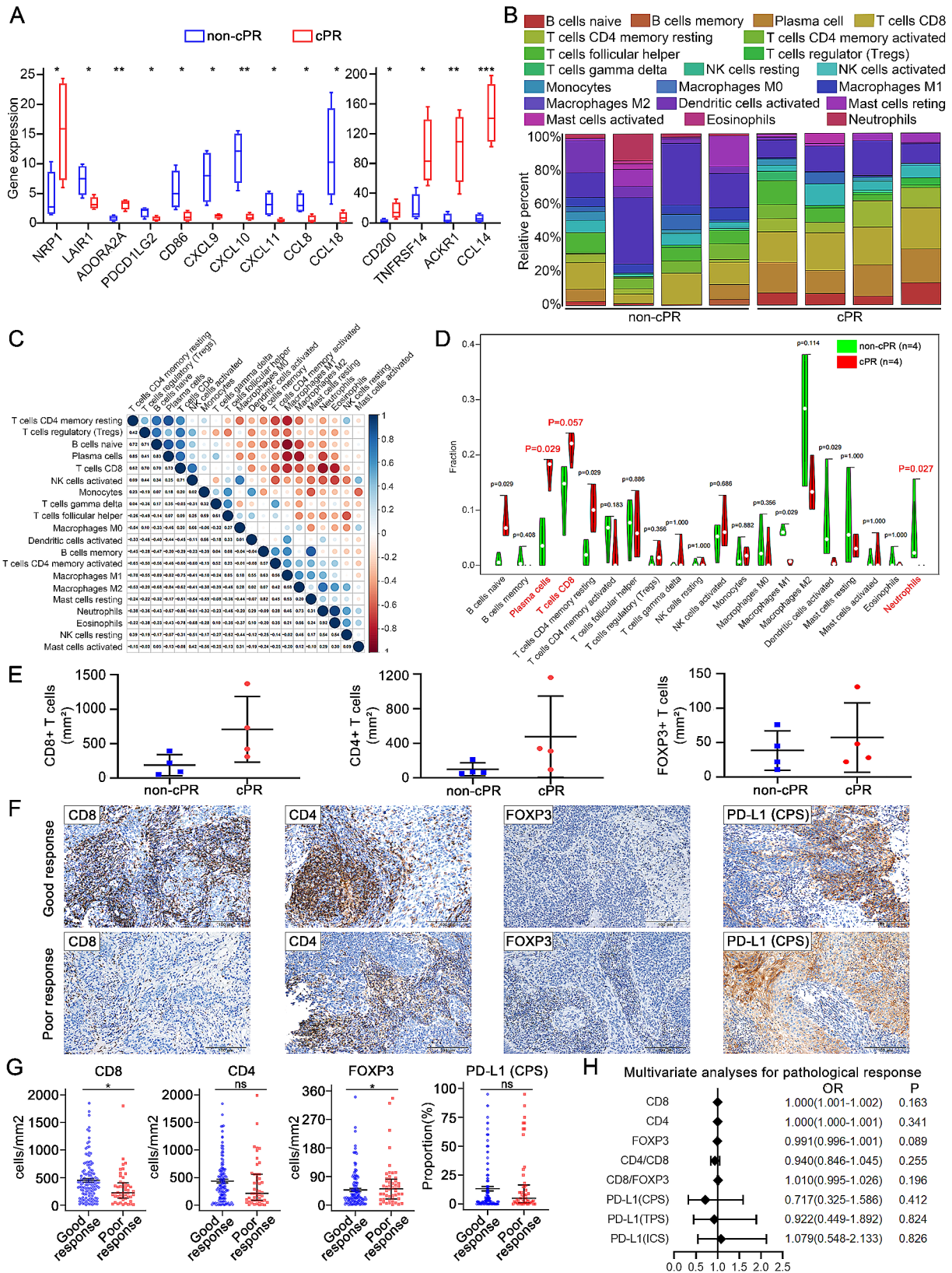


Fig. 3 (See legend on next page.)

(See figure on previous page.)

Fig. 3 A comparison of immune cell infiltration in 4 cPR samples and 4 non-cPR samples (The viable tumor of 4 non-cPR samples is 20%, 70%, 90% and 95%, respectively). (A) Differences in chemokine and chemokine receptor expression in cPR group compared with non-cPR group. * $P < 0.05$, ** $P < 0.01$, *** $P < 0.001$. (B) The distribution of immune cells among cPR and non-cPR samples. (C) Correlation among variable immune cells in cPR and non-cPR samples. (D) Infiltration immune cell analysis between cPR groups and non-cPR groups. (E) Differences of CD8, CD4 as well as FOXP3 IHC staining in cPR and non-cPR samples. (F) Representative images of CD8+, CD4+, FOXP3+TILs and PD-L1 expression based on CPS pre-treatment in good response group and poor response group. (G) Box plots show the differences of densities of CD8+, CD4+, FOXP3+TILs and score of PD-L1 expression based on CPS pre-treatment in good response group compared with poor response group. * $P < 0.05$; ns, no significance. (H) Multivariate analyses of immune markers pre-treatment for pathological response are shown in forest map. cPR, complete pathological response; PD-L1, programmed cell death ligand 1; CPS, combined positive score

CD4+T cells density and PD-L1 expression between the two groups (Table 2; Fig. 3G). However, PD-L1 (CPS) was positively expressed in 74.6% (100/134) of samples in good response group, PD-L1 (TPS) in 70.9% (95/134) and PD-L1 (ICS) in 66.3% (89/134). Similarly, we found the 80.4% (41/51) of samples in poor response group expressed PD-L1 (CPS), 72.5% (37/51) expressed PD-L1 (TPS) and 64.7% (33/51) expressed PD-L1 (ICS). Despite conducting a multivariate logistic regression analysis on pre-treatment immune markers for pathological response, no significant results were observed (Fig. 3H). These results substantiated that elevated TILs were correlated with a favorable pathological response to NACT.

Stromal type of post-treatment significantly correlated with LACC's prognosis

Subsequently, our primary focus shifted to the assessment of the tumor bed stroma in resection tissues post-NACT. As illustrated in Fig. 4A-B, the 185 LACCs were subclassified into four stromal types: 53 inflammatory type, 59 fibrotic type, 5 necrotic type and 67 intermediate type. Therapeutically induced histological features were discerned in resection tissues, exemplified in Fig. 4C. Inflammatory stroma manifested as infiltration by lymphocytes, plasma cells, neutrophils, eosinophils, foamy cells, multinucleated giant cells, cholesterol clefts and calcification. Fibrotic encompassed both loose or myxoid connective tissue and dense hyalinized connective tissue. Additionally, pronounced vascularity proliferation was evident in the stroma. Noteworthy correlations were identified between pathological response and select therapy-related histological features, including neutrophils ($p=0.016$), eosinophils ($p=0.041$), foamy cells ($p=0.021$) and necrosis ($p<0.0001$) (Fig. 4D). Foamy cells were more prevalent in patients with good pathological response while neutrophils, eosinophils and necrosis were more frequent in the poor response group. Multivariate analysis further identified foamy cells (HR=0.409, 95%CI=0.207–0.808, $p=0.010$) and hyalinized connective tissue (HR=2.195, 95%CI=1.110–4.341, $p=0.024$) as independent factors for DFS (Supplementary Figure S2B).

Subsequent Kaplan-Meier analysis was conducted to assess the impact of pathological response and stromal type post-NACT on the prognosis of LACC patients

(Fig. 4E). Good pathological response correlated with better OS ($p=0.006$) and DFS ($p=0.005$). Concerning stromal type, patients with inflammatory type and intermediate type exhibited significantly longer OS and DFS, but there was no significant difference between them. Remarkably, the fibrotic type displayed an intermediate prognosis, while necrotic type had the poorest prognosis for both DFS and OS (both $p<0.0001$). Crucially, multivariate analysis established stromal type as an independent prognostic factor for both OS (HR=3.749, 95%CI=1.861–7.552, $p=0.004$) and DFS (HR=4.719, 95%CI=2.634–8.456, $p<0.0001$) in LACC (Table 3).

Association of TIME with pathological response to NACIT in LACC

To enhance our understanding of the evaluation of pathological response post-NACT in LACC patients, we extended our examination to the NACIT cohort. Baseline characteristics of the 7 patients undergoing NACIT are detailed in Supplementary Tables 3 and Supplementary Figure S3A, encompassing individuals aged 26 to 66, with follow-up periods ranging from 1 to 15 months. Notably, 85.7% (6/7) of the cohort exhibited good pathological response, comprising 1 case of cPR, 4 cases of mPR and 1 case of pPR. It is noteworthy that the residual viable tumor in all 6 good response cases were all $\leq 15\%$. Only one case was assigned to nPR, with a residual viable tumor of 65%. Importantly, no recurrence or mortality was observed in any of the 7 cases. The pPR case revealed lymph node metastatic and nerve bundle invasion with a residual viable tumor of 15%. Similarly, the nPR case exhibited lymph node metastatic and vascular invasion. Conversely, the remaining 5 cases displayed neither lymph node metastatic nor vascular or nerve bundle invasion. Representative H&E stain and IHC images were presented in Supplementary Figure S3B. PD-L1 (CPS) positive was observed in all cases, particularly with relatively high expression in cPR and mPR cases. Furthermore, 87.5% (5/6) of the good response cases presented abundant stromal TILs pre-treatment, including CD8+T cells and CD4+T cells.

Table 2 Correlation of immune markers pre-treatment and pathological response.

Variables	Total	Good response (cPR, mPR, pPR) (N, %)	Poor response (nPR) (N, %)	P
CD8 density (cells/mm²)	185	450.3 ± 32.6	356.7 ± 65.1	0.015
CD4 density (cells/mm²)	185	436.9 ± 33.8	374.3 ± 58.8	0.151
FOXP3 density (cells/mm²)	185	47.7 ± 4.8	65.2 ± 10.0	0.036
CD4/CD8				0.010
>2.17	27(14.6)	14(10.4)	13(25.5)	
≤2.17	158(85.4)	120(89.6)	38(74.5)	
CD8/FOXP3				<0.000
>5.24	120(64.9)	99(73.9)	21(41.2)	
≤5.24	65(35.1)	35(26.1)	30(58.8)	
PD-L1 (CPS)				0.410
Positive	141(76.2)	100(74.6)	41(80.4)	
Negative	44(23.8)	34(25.4)	10(19.6)	
PD-L1 (TPS)				0.824
Positive	132(71.4)	95(70.9)	37(72.5)	
Negative	53(28.6)	39(29.1)	14(27.5)	
PD-L1 (IPS)				0.826
Positive	122(65.9)	89(66.3)	33(64.7)	
Negative	63(34.1)	45(33.6)	18(35.3)	

NACT, neoadjuvant chemotherapy; cPR, complete pathological response; mPR, major pathological response; pPR, partial pathological response; nPR, no pathological response; PD-L1, programmed cell death ligand 1; CPS, combined positive score; IPS, immune cell proportion score; TPS, tumor cell proportion score

Discussion

To date, a standard pathological evaluation system for cervical cancer remains elusive. While there is a general consensus to defining cPR, the categorization of non-complete response varies across studies [19]. Previous studies have typically classified pathological response into different grades based on the residual tumor size or invasive depth [19]. In our approach, we quantified the percentage of residual viable tumor in the cervical primary region, drawing inspiration from definitions in lung cancer (mPR) [27] and melanoma (pPR and nPR) [21]. Consequently, we devised a four-tiered pathological response evaluation system for cervical cancer post-NACT, encompassing cPR, mPR, pPR and nPR. This system, not reliant on tumor size or invasive depth, offers a more nuanced reflection of tumor overall state and treatment response. Importantly, our pathological system exhibited a robust correlation with the RECIST in radiological response assessment. Pathological assessment can additionally reveal inflammatory or fibrotic stroma that are challenging to discern through CT scans. The synergistic application of both CT imaging and pathological assessment may improve the precision in evaluating the effectiveness of neoadjuvant therapy.

The immune microenvironment emerges as intricately linked to the pathological response to NACT [28]. Stromal TILs have been recognized as a prognostic indicator and a predictor of pathological response post-NACT, playing a pivotal role in tumor immunity [11, 29, 30]. Aligning with prior studies, we found that heightened expression levels of stromal TILs correlated with a more favorable pathological response. Our study also identified the T cell proliferation pathway, particularly evaluated expression of CD8+T cells, as crucial for achieving cPR. This finding was subsequently validated through IHC staining of 185 LACC biopsy specimens. The increased presence of CD8+T cells in biopsies appears indicative of a more favorable pathological response post-NACT. Tumor infiltrating CD8+T cells are widely recognized as pivotal guardians against tumorigenesis, with their ability to mount a robust anti-tumor response. Conversely, FOXP3+T cells play a regulatory role by impeding the proliferation and activation of CD8+T cells, as evidenced by pertinent studies [9]. An elevated CD8/FOXP3 ratio emerges as a notable prognostic indicator for enhanced survival across diverse cancer types, including rectal cancer, esophageal squamous cell cancer, lung adenocarcinoma and cervical cancer [9, 31–33]. It may be the balance or interaction between CD8+and FOXP3+T cells in the tumor microenvironment rather than the quantity of TILs alone, determines clinical outcomes. In this study, we found that a high infiltration of CD8+T cells coupled with low levels of FOXP3+T cells in the tumor stroma may aid in selecting patients who are clinically responsive to chemotherapy, undergoing the influence of host pretreatment immune status on chemotherapy effectiveness. Additionally, in the NACIT cohort, 6 out of 7 LACC patients exhibited a favorable pathological response alongside a high level of immune cell infiltration or positive PD-L1 expression in biopsy samples. This may indicate the great potential of immunotherapy in LACC. Indeed, the co-expression of PD-L1 and TILs have been reported in various cancers [10, 34]. When PD-L1 on tumor tissue binds to its ligand PD-1, it triggers an immunosuppressive signal, hindering immune cells to attack tumor. Elevated levels of TILs suggest an activated immune environment within the body. When alleviating PD-L1 inhibition on TILs, more immune cells can be activated to identify and eliminate tumor cells [35, 36]. Hence, the utilization of immune checkpoint inhibitors, such as PD-L1/PD-1 blockers, may yield a potent and efficacious response in cases where PD-L1 and TILs are co-expressed. Nevertheless, the potential of PD-L1 and TILs as biomarkers for predicting treatment response and prognosis in cervical cancer requires further exploration.

Currently, studies on cervical cancer post-NACT predominantly focus on tumor staging, histological types

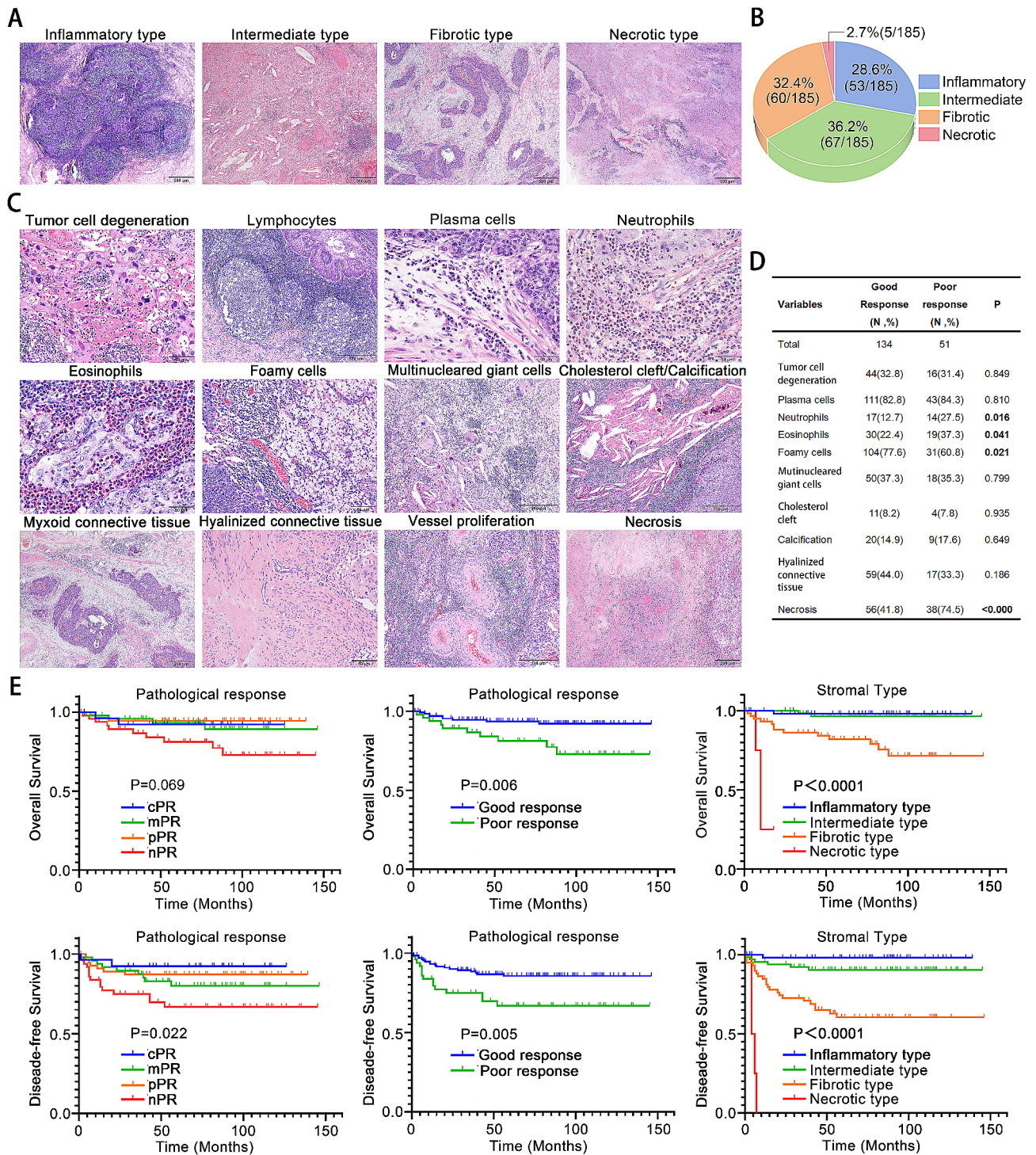


Fig. 4 (A) Representative images of 4 stromal types. (B) Fractions of 4 stromal types. (C) Representative images of therapy-related histological features. Lymphocytes, plasma cells, neutrophils, eosinophils, foamy cells, multinucleated giant cells, cholesterol cleft and calcification are classified into inflammatory stroma. Loose or myxoid connective tissue, dense hyalinized connective tissue and vessel proliferation are classified into fibrotic stroma. (D) Correlations between therapy-related histological features and pathological response. (E) Kaplan-Meier survival curves for DFS and OS according to pathological response and stromal type post treatment. DFS, disease-free survival; OS, overall survival

Table 3 Univariate and multivariate analyses for DFS and OS.

Variables	Univariate analyses		Multivariate analyses	
	HR (95%CI)	P	HR (95%CI)	P
OS				
Age (> 48 years vs. ≤48 years)	5.127(1.502–17.508)	0.009	5.804(1.682–20.030)	0.005
FIGO Stage (IB3 vs. IIA2-IVA)	2.405(0.874–6.623)	0.089		
HPV (Positive vs. Negative)	1.377(0.663–2.859)	0.391		
Tumor size (pre) (> 5.9cm vs. ≤5.9cm)	0.911(0.304–2.728)	0.868		
Histologic type (SCCA vs. others)	0.830(0.111–6.211)	0.856		
Differentiation (Well + Moderate vs. Poor)	0.812(0.338–1.954)	0.642		
Stromal invasion level (< 1/3 vs. 1/3–2/3 vs.>2/3)	2.500(1.377–4.540)	0.003		
Parametrium invasion (Yes vs. No)	6.735(2.233–20.310)	0.001	4.903(1.347–17.851)	0.016
Lymph node metastatic (Yes vs. No)	6.035(2.494–14.602)	<0.000		
Vascular invasion (Yes vs. No)	7.123(2.905–17.467)	<0.000	5.764(2.185–15.206)	<0.000
Nerve bundle invasion (Yes vs. No)	2.490(0.575–10.778)	0.222		
Pathological response (Good response vs. Poor response)	0.341(0.142–0.820)	0.016		
Stromal type (Inflammatory vs.Intermediate vs.Fibrotic vs.Necrotic)	6.353(2.867–14.081)	<0.000	3.749(1.861–7.552)	0.004
DFS				
Age (> 48 years vs. ≤ 48 years)	1.406(0.704–2.808)	0.334		
FIGO Stage (IB3 vs. IIA2-IVA)	1.430(0.708–2.890)	0.319		
HPV status (Positive vs. Negative)	2.514(0.330–19.120)	0.373		
Tumor size (pre) (> 5.9cm vs. ≤5.9cm)	0.692(0.287–1.666)	0.411		
Histologic type (SCCA vs. others)	0.930(0.223–3.876)	0.921		
Differentiation (Well + Moderate vs. Poor)	0.694(0.357–1.350)	0.282		
Stromal invasion level (< 1/3 vs. 1/3–2/3 vs.>2/3)	2.233(1.451–3.437)	<0.000		
Parametrium invasion (Yes vs. No)	3.426(1.205–9.739)	0.021		
Lymph node metastatic (Yes vs. No)	6.097(3.096–12.008)	<0.000		
Vascular invasion (Yes vs. No)	5.973(3.037–11.749)	<0.000	4.214(2.098–8.467)	<0.000
Nerve bundle invasion (Yes vs. No)	5.727(2.340–14.018)	<0.000		
Pathological response (Good response vs. Poor response)	0.414(0.210–0.815)	0.011		
Stromal type (Inflammatory vs.Intermediate vs.Fibrotic vs.Necrotic)	5.696(3.101–10.464)	<0.000	4.719(2.634–8.456)	<0.000

HR, hazard ratio; OS, overall survival; DFS, disease-free survival; FIGO, International Federation of Gynecology and Obstetrics; HPV, human papilloma virus; NACT, neoadjuvant chemotherapy; SCCA, squamous cell carcinoma

and conventional pathological risk factors like lymphatic vascular invasion [28, 37]. However, the morphological alterations of tumor cells and stroma and their impact on prognosis remain underexplored. Our study directs attention to the stroma, encompassing inflammation, fibrosis, and necrosis. Tumor-associated inflammatory infiltration has long been recognized as a host response and a crucial factor in anti-tumor activity. Notably, good responders exhibit dense TILs and plasma cells in post-treatment excised specimens, pivotal for bolstering the anti-tumor response [17]. Other immune cell subsets, including Tregs and M2 macrophages, have also been implicated in promoting tissue repair, suggesting a complex interplay between specific immune cell subsets, tumor cell death and tissue repair [38–40]. Our findings suggest that a broader inflammation in the tumor bed may correlate with a more favorable prognostic assessment, warranting further exploration of treatment options aimed at enhancing the host immune response in patients. In addition to inflammatory infiltration, fibrosis and necrosis represent alternative forms

of tumor regression. Some studies have explored these aspects in soft tissue tumors, with necrosis post-NACT considered an adverse prognostic factor, while tumor fibrosis seems to reflect a reparative response to initial tumor necrosis [41, 42]. The collagen fibers, serve as the primary components of the extracellular matrix, origin from cancer-associated fibroblasts (CAFs). Chemotherapy may activate CAFs and prompt the accumulation of collagen fibers within the stroma. This may facilitate the formation of a natural barrier, leading to immune resistance and influencing subsequent anti-tumor therapies. Consequently, it may contribute to a poor prognosis of patients [43, 44]. Our study underscores that the stromal type post-treatment emerges as an independent prognostic factor in LACC patients, which may offer guidance for prognosis and clinical decisions. However, the actual prognostic impact may hinge on the interplay of multiple factors. It is not advisable to rely solely on this factor for making medical decision. Rather, it should be assessed in conjunction with other pertinent clinical parameters.

Despite developing a straightforward and prognostically significant system for grading the response of LACC patients to NACT, our study has limitations. The retrospective nature of our pathological response evaluation system calls for more robust evidence through a meticulous and randomized prospective clinical study. Moreover, as all specimens originated from a single center, potential selection bias arises, necessitating further validated of our results in multi-center studies with a larger sample size.

Abbreviations

CCRT	Concurrent chemoradiotherapy
LACC	Locally advanced cervical cancer
NACT	Neoadjuvant chemotherapy
TILs	Tumor-infiltrating lymphocytes
TILV	Tumor infiltrating lymphocytes volume
SYSUCC	Sun Yat-sen University Cancer Center
FIGO	International Federation of Gynecology and Obstetrics
CT	Pelvic computed tomography
PD	Progressive disease
SD	Stable disease
PR	Partial response
CR	Tumor complete resolution
cPR	Complete pathological response
mPR	Major pathological response
pPR	Partial pathological response
nPR	No pathological response
DEG	Differentially expressed genes
GO	Gene ontology
FDR	False Discovery Rates
HE	Hematoxylin-eosin staining
IHC	Immunohistochemistry
FOXP3	Forkhead box protein P3
DAB	Diaminobenzidine tetrahydro-chloride
PD-L1	Programmed death-ligand 1
CPS	Combined positive score
TPS	Tumor proportion score
IPS	Immune cell proportion score
ROC	Receiver Operating Characteristic
TIME	Tumor immune microenvironment
KEGG	Kyoto Encyclopedia of Genes and Genomes
HPV	Human papilloma virus
NA	Not available
LDH	Lactate dehydrogenase
SCC	Squamous cell carcinoma antigen
CEA	Carcinoembryonic antigen
SCCA	Squamous cell carcinoma
AC	Adenocarcinoma
ASC	Adenosquamous carcinoma
NEC	Neuroendocrine carcinoma
LN1	Lymph node metastatic
HR	Hazard ratio
OS	Overall survival
DFS	Disease-free survival
OR	Odds ratio
NACT	Neoadjuvant chemotherapy combined with immunotherapy

Supplementary Information

The online version contains supplementary material available at <https://doi.org/10.1186/s12967-024-05482-3>.

Supplementary Material 1

Acknowledgements

This work was supported by grants from the National Natural Science Foundation of China (No. 82072853).

Author contributions

Conception and design: Rong-Zhen Luo and Li-Li Liu. Performing experiments: Li-Jun Wei, Hai-Xia Yang, and Xia Yang. Drafting of the article: Li-Li Liu and Li-Jun Wei. Acquisition and interpretation of data, review, editing, and approval of the manuscript: all authors.

Data availability

The datasets used or analyzed during the current study are available from the corresponding author on reasonable request.

Declarations

Ethics approval and consent to participate

Approval of the research protocol by an institutional review board: Our study was approved by the Institutional Ethical Board of Sun Yat-sen University Cancer Center. Informed Consent: All Informed consent was obtained from all subjects.

Consent for publication

Not applicable.

Competing interests

The authors have declared that no competing interests exists.

Received: 12 April 2024 / Accepted: 3 July 2024

Published online: 14 July 2024

References

1. Sung H, Ferlay J, Siegel RL, et al. Global Cancer statistics 2020: GLOBOCAN estimates of incidence and Mortality Worldwide for 36 cancers in 185 countries. *Cancer J Clin*. 2021;71(3):209–49. <https://doi.org/10.3322/caac.21660>.
2. Minig L. Different strategies of treatment for uterine cervical carcinoma stage IB2-IB. *World J Clin Oncol*. 2014;5(2):86–92. <https://doi.org/10.5306/wjco.v5.i2.86>.
3. Kfoury CFA, Lombardi W, Romania MCFN, et al. Fatores prognósticos De resposta à quimioterapia em tumores avançados do colo uterino: o papel da neangiogênese. *Revista do Colégio Brasileiro De Cirurgiões*. 2019;46(1). <https://doi.org/10.1590/0100-6991e-20192077>.
4. Li J, Liu H, Li Y, et al. Comparison of outcomes and side effects for neoadjuvant chemotherapy with weekly cisplatin and paclitaxel followed by chemoradiation vs. chemoradiation alone in stage IIB–IVA cervical cancer: study protocol for a randomized controlled trial. *Trials*. 2022;23(1). <https://doi.org/10.1186/s13063-021-05986-z>.
5. Huang Y, Chen L, Cai J, et al. Neoadjuvant chemotherapy followed by radical surgery reduces radiation therapy in patients with stage IB2 to IIA2 cervical cancer. *World J Surg Oncol*. 2022;20(1):264. <https://doi.org/10.1186/s12957-022-02731-x>.
6. Zhu Y, Yang J, Zhang X, et al. Acquired treatment response from neoadjuvant chemotherapy predicts a favorable prognosis for local advanced cervical cancer. *Medicine*. 2018;97(17):e0530. <https://doi.org/10.1097/md.00000000000010530>.
7. Federico A, Anchora LP, Gallotta V, et al. Clinical impact of pathologic residual tumor in locally Advanced Cervical Cancer patients managed by Chemoradiotherapy followed by radical surgery: a large, Multicenter, Retrospective Study. *Ann Surg Oncol*. 2022;29(8):4806–14. <https://doi.org/10.1245/s10434-022-11583-4>.
8. Park DC, Suh MJ, Yeo SG. Neoadjuvant Paclitaxel and Cisplatin in Uterine Cervical Cancer. *Int J Gynecol Cancer*. 2009;19(5):943–7. <https://doi.org/10.1111/IGC.0b013e3181a23c2e>.
9. Liang Y, Lü W, Zhang X, et al. Tumor-infiltrating CD8+ and FOXP3+ lymphocytes before and after neoadjuvant chemotherapy in cervical cancer. *Diagn Pathol*. 2018;13(1):93. <https://doi.org/10.1186/s13000-018-0770-4>.
10. D'Alessandris N, Palaia I, Pernazza A, et al. PD-L1 expression is associated with tumor infiltrating lymphocytes that predict response to NACT in

- squamous cell cervical cancer. *Virchows Arch.* 2021;478(3):517–25. <https://doi.org/10.1007/s00428-020-02922-5>.
11. Ochi T, Bianchini G, Ando M, et al. Predictive and prognostic value of stromal tumour-infiltrating lymphocytes before and after neoadjuvant therapy in triple negative and HER2-positive breast cancer. *Eur J Cancer.* 2019;118:41–8. <https://doi.org/10.1016/j.ejca.2019.05.014>.
 12. Zhang L, Wang Xi, Zhang S. Tumor-infiltrating lymphocyte volume is a better predictor of neoadjuvant therapy response and overall survival in triple-negative invasive breast cancer. *Hum Pathol.* 2018;80:47–54. <https://doi.org/10.1016/j.humpath.2018.05.024>.
 13. Ogston KN, Miller ID, Payne S, et al. A new histological grading system to assess response of breast cancers to primary chemotherapy: prognostic significance and survival. *Breast.* 2003;12(5):320–7. [https://doi.org/10.1016/s0960-9776\(03\)00106-1](https://doi.org/10.1016/s0960-9776(03)00106-1).
 14. Mandard A-M, Dalibard F, Mandard J-C, et al. Pathologic assessment of tumor regression after preoperative chemoradiotherapy of esophageal carcinoma. Clinicopathological correlations. *Cancer.* 1994;73(11):2680–6. [https://doi.org/10.1002/1097-0142\(19940601\)73:11%3C2680::Aid-cncr2820731105%3E3.0.Co;2-c](https://doi.org/10.1002/1097-0142(19940601)73:11%3C2680::Aid-cncr2820731105%3E3.0.Co;2-c).
 15. Böhm S, Faruqi A, Said I, et al. Chemotherapy response score: development and validation of a system to quantify histopathologic response to Neoadjuvant Chemotherapy in Tubo-Ovarian High-Grade Serous Carcinoma. *J Clin Oncol.* 2015;33(22):2457–63. <https://doi.org/10.1200/jco.2014.60.5212>.
 16. Travis WD, Dacic S, Wistuba I, et al. IASLC Multidisciplinary recommendations for Pathologic Assessment of Lung Cancer resection specimens after neoadjuvant therapy. *J Thorac Oncol.* 2020;15(5):709–40. <https://doi.org/10.1016/j.jtho.2020.01.005>.
 17. Cottrell TR, Thompson ED, Forde PM, et al. Pathologic features of response to neoadjuvant anti-PD-1 in resected non-small-cell lung carcinoma: a proposal for quantitative immune-related pathologic response criteria (irPRC). *Ann Oncol.* 2018;29(8):1853–60. <https://doi.org/10.1093/annonc/mdy218>.
 18. Zannoni GF, Vellone VG, Carbone A. Morphological effects of Radiochemotherapy on Cervical Carcinoma. *Int J Gynecol Pathol.* 2008;27(2):274–81. <https://doi.org/10.1097/PGP.0b013e31815b1263>.
 19. Zannoni GF, Travaglini A, Raffone A et al. Depth of Stromal Invasion as the Most Prognostically Relevant Regression System in Locally Advanced Cervical Cancer after Neoadjuvant Treatment: A Systematic Review and Meta-Analysis Grading. *Diagnostics* 2021; 11(10):1772. <https://doi.org/10.3390/diagnostics11101772>.
 20. Eisenhauer EA, Therasse P, Bogaerts J, et al. New response evaluation criteria in solid tumours: revised RECIST guideline (version 1.1). *Eur J Cancer.* 2009;45(2):228–47. <https://doi.org/10.1016/j.ejca.2008.10.026>.
 21. Tetzlaff MT, Messina JL, Stein JE, et al. Pathological assessment of resection specimens after neoadjuvant therapy for metastatic melanoma. *Ann Oncol.* 2018;29(8):1861–8. <https://doi.org/10.1093/annonc/mdy226>.
 22. Hendry S, Salgado R, Gevaert T, et al. Assessing tumor-infiltrating lymphocytes in solid tumors: a practical review for pathologists and proposal for a standardized method from the International Immuno-Oncology biomarkers Working Group: part 2: TILs in Melanoma, gastrointestinal Tract carcinomas, non-small cell lung carcinoma and mesothelioma, endometrial and ovarian carcinomas, squamous cell carcinoma of the Head and Neck, Genitourinary Carcinomas, and primary brain tumors. *Adv Anat Pathol.* 2017;24(6):311–35. <https://doi.org/10.1097/pap.000000000000161>.
 23. Ritchie ME, Phipson B, Wu D, et al. Limma powers differential expression analyses for RNA-sequencing and microarray studies. *Nucleic Acids Res.* 2015;43(7):e47. <https://doi.org/10.1093/nar/gkv007>.
 24. Wu T, Hu E, Xu S, et al. clusterProfiler 4.0: a universal enrichment tool for interpreting omics data. *Innov.* 2021;2(3):100141. <https://doi.org/10.1016/j.xinn.2021.100141>.
 25. Newman AM, Liu CL, Green MR, et al. Robust enumeration of cell subsets from tissue expression profiles. *Nat Methods.* 2015;12(5):453–7. <https://doi.org/10.1038/nmeth.3337>.
 26. Schildhaus HU. Der prädiktive Wert Der PD-L1-Diagnostik. *Pathologe.* 2018;39(6):498–519. <https://doi.org/10.1007/s00292-018-0507-x>.
 27. Vos JL, Elbers JBW, Krijgsman O, et al. Neoadjuvant immunotherapy with nivolumab and ipilimumab induces major pathological responses in patients with head and neck squamous cell carcinoma. *Nat Commun.* 2021;12(1). <https://doi.org/10.1038/s41467-021-26472-9>.
 28. Meng Y, Liang H, Hu J, et al. PD-L1 expression correlates with Tumor infiltrating lymphocytes and response to neoadjuvant Chemotherapy in Cervical Cancer. *J Cancer.* 2018;9(16):2938–45. <https://doi.org/10.7150/jca.22532>.
 29. Russo L, Maltese A, Betancourt L, et al. Locally advanced breast cancer: Tumor-infiltrating lymphocytes as a predictive factor of response to neoadjuvant chemotherapy. *Eur J Surg Oncol.* 2019;45(6):963–8. <https://doi.org/10.1016/j.ejso.2019.01.222>.
 30. Palaia I, Tomao F, Di Pinto A, et al. Response to Neoadjuvant Chemotherapy in locally Advanced Cervical Cancer: the role of Immune-related factors. *Vivo.* 2021;35(2):1277–83. <https://doi.org/10.21873/invivo.12379>.
 31. Schnellhardt S, Hirneth J, Büttner-Herold M, et al. The Prognostic Value of FoxP3+ tumour-infiltrating lymphocytes in rectal Cancer depends on Immune Phenotypes defined by CD8+ cytotoxic T cell density. *Front Immunol.* 2022;13:781222. <https://doi.org/10.3389/fimmu.2022.781222>.
 32. Zhu Y, Li M, Mu D, et al. CD8+/FOXP3+ ratio and PD-L1 expression associated with survival in pT3N0M0 stage esophageal squamous cell cancer. *Oncotarget.* 2016;7(44):71455–65. <https://doi.org/10.18632/oncotarget.12213>.
 33. Kinoshita F, Takada K, Yamada Y, et al. Combined evaluation of Tumor-infiltrating CD8+ and FoxP3+ lymphocytes provides Accurate Prognosis in Stage IA Lung Adenocarcinoma. *Ann Surg Oncol.* 2020;27(6):2102–9. <https://doi.org/10.1245/s10434-019-08029-9>.
 34. Yagi T, Baba Y, Ishimoto T, et al. PD-L1 expression, tumor-infiltrating lymphocytes, and clinical outcome in patients with surgically resected esophageal Cancer. *Ann Surg.* 2019;269(3):471–8. <https://doi.org/10.1097/SLA.0000000000002616>.
 35. Mimura K, Teh JL, Okayama H, et al. PD-L1 expression is mainly regulated by interferon gamma associated with JAK-STAT pathway in gastric cancer. *Cancer Sci.* 2018;109(1):43–53. <https://doi.org/10.1111/cas.13424>.
 36. Deng C, Li Z, Guo S, et al. Tumor PD-L1 expression is correlated with increased TILs and poor prognosis in penile squamous cell carcinoma. *Oncimmunology.* 2017;6(2):e1269047. <https://doi.org/10.1080/2162402X.2016.1269047>.
 37. Couvreur K, Naert E, De Jaeghere E, et al. Neo-adjuvant treatment of adenocarcinoma and squamous cell carcinoma of the cervix results in significantly different pathological complete response rates. *BMC Cancer.* 2018;18(1):1101. <https://doi.org/10.1186/s12885-018-5007-0>.
 38. Kumar S, Calianese D, Birge RB. Efferocytosis of dying cells differentially modulate immunological outcomes in tumor microenvironment. *Immunol Rev.* 2017;280(1):149–64. <https://doi.org/10.1111/imr.12587>.
 39. Fuchs Y, Steller H. Live to die another way: modes of programmed cell death and the signals emanating from dying cells. *Nat Rev Mol Cell Biol.* 2015;16(6):329–44. <https://doi.org/10.1038/nrm3999>.
 40. Green JA, Arpaia N, Schizas M, et al. A nonimmune function of T cells in promoting lung tumor progression. *J Exp Med.* 2017;214(12):3565–75. <https://doi.org/10.1084/jem.20170356>.
 41. Cates JMM. Histologic response to Neoadjuvant Therapy is not predictive of favorable outcomes in high-grade Pleomorphic Soft tissue sarcoma. *Am J Surg Pathol.* 2019;43(4):564–72. <https://doi.org/10.1097/pas.0000000000001214>.
 42. Gannon NP, Stemm MH, King DM, et al. Pathologic necrosis following neoadjuvant radiotherapy or chemoradiotherapy is prognostic of poor survival in soft tissue sarcoma. *J Cancer Res Clin Oncol.* 2019;145(5):1321–30. <https://doi.org/10.1007/s00432-019-02885-4>.
 43. Naik A, Leask A. Tumor-associated fibrosis impairs the response to immunotherapy. *Matrix Biol.* 2023;119:125–40. <https://doi.org/10.1016/j.matbio.2023.04.002>.
 44. Kim DK, Jeong J, Lee DS, et al. PD-L1-directed PIGF/VEGF blockade synergizes with chemotherapy by targeting CD141+ cancer-associated fibroblasts in pancreatic cancer. *Nat Commun.* 2022;13(1):6292. <https://doi.org/10.1038/s41467-022-33991-6>.

Publisher's Note

Springer Nature remains neutral with regard to jurisdictional claims in published maps and institutional affiliations.